

## Flexible room-temperature NO<sub>2</sub> gas sensors based on carbon nanotubes/reduced graphene hybrid films

Hu Young Jeong,<sup>1</sup> Dae-Sik Lee,<sup>2</sup> Hong Kyw Choi,<sup>2,3</sup> Duck Hyun Lee,<sup>1</sup> Ji-Eun Kim,<sup>1</sup> Jeong Yong Lee,<sup>1</sup> Won Jong Lee,<sup>1</sup> Sang Ouk Kim,<sup>1</sup> and Sung-Yool Choi<sup>2,3,a)</sup>

<sup>1</sup>Department of Materials Science and Engineering, KAIST, Daejeon 305-701, Republic of Korea

<sup>2</sup>Electronics and Telecommunications Research Institute (ETRI), Daejeon 305-700, Republic of Korea

<sup>3</sup>Department of Advanced Device Technology, University of Science and Technology (UST), Daejeon 305-333, Republic of Korea

(Received 15 February 2010; accepted 29 April 2010; published online 25 May 2010)

We present a flexible room temperature NO<sub>2</sub> gas sensor consisting of vertical carbon nanotubes (CNTs)/reduced graphene hybrid film supported by a polyimide substrate. The reduced graphene film alone showed a negligible sensor response, exhibiting abnormal N–P transitions during the initial NO<sub>2</sub> injection. A hybrid film, formed by the growth of a vertically aligned CNT array (with CNTs 20 μm in length) on the reduced graphene film surface, exhibited remarkably enhanced sensitivities with weak N–P transitions. The increase in sensitivity was mainly attributed to the high sensitivity of the CNT arrays. The outstanding flexibility of the reduced graphene films ensured stable sensing performances in devices submitted to extreme bending stress. © 2010 American Institute of Physics. [doi:10.1063/1.3432446]

Graphene, a one-atom-thick two-dimensional sheet of *sp*<sup>2</sup>-hybridized carbon atoms, shows tremendous promise for advanced nanoelectronic devices.<sup>1,2</sup> Owing to its unique electrical properties and large surface area, graphene is considered a viable candidate for high performance gas sensing element. Recently, mechanically exfoliated monolayer graphene sheet, was employed in gas sensing devices and demonstrated exceptionally low detection noise levels at room temperature.<sup>3</sup> Although this report suggested the great potential of graphene for chemical sensors, mass-production of graphene sheet and its integration into device architecture remained challenging issue for viable sensor fabrication. More recently, chemically exfoliated graphene sheets have been used for NO<sub>2</sub> sensors.<sup>4,5</sup> These approaches accomplished low-cost methods for large-scale fabrication. Nevertheless the sensing response was relatively weak and unstable for high performance sensing applications.

On the other hands, carbon nanotubes (CNTs) have also attracted intensive research interest due to their potential for the detection of various gaseous species.<sup>6,7</sup> Even though the gas sensing response of CNTs is larger and more rapid than that of graphene, the integration onto flexible substrates for the application under an extremely flexed condition is still unsolved because of the imperfect contact with metal electrodes.

In this letter, therefore, we introduce an advanced carbon-based gas sensing material consisted of CNTs/graphene hybrid film. This material synergistically comprises the high gas sensitivity of CNTs with mechanical flexibility<sup>2</sup> of graphene film substrate, which is used as a connecting medium between metal electrodes (Au) and CNT arrays. In particular, the high flexibility of bottom graphene substrate ensures facile integration of this hybrid film into sensing device structure and stable gas sensitivity even under extreme bending.

The CNTs/reduced graphene hybrid films were grown on a 500 nm thick SiO<sub>2</sub> layer supported on a Si wafer, as described previously.<sup>8</sup> In brief, a 7 nm thick graphene oxide film was spin-coated from an aqueous suspension of graphene oxide, and the nanopatterned iron catalyst was prepared by block copolymer lithography. Subsequently, vertical CNTs were grown by plasma-enhanced chemical vapor deposition. The reduced graphene only films were prepared by subjecting the spin-coated graphene oxide films to thermal heat treatment at 600 °C in the presence of a mixture of hydrogen and ammonia gas. Both films were detached from the Si substrates by wet etching using a dilute HF solution then transferred to Au/polyimide flexible substrates. The gas sensing properties were characterized using a digital multimeter (HP 3458A) and a dc power supply (HP E3610A). N<sub>2</sub> or N<sub>2</sub>/NO<sub>2</sub> gas mixtures fixed at a flow rate of 1000 SCCM (SCCM denotes cubic centimeter per minute at STP) were injected into a glass chamber using mass flow controllers, and all measured data were recorded on a desktop computer.

The schematic illustration of our flexible NO<sub>2</sub> gas sensor based on the CNTs/reduced graphene hybrid films is shown in Fig. 1(a). The active cell consisted of polyimide substrate, Au electrodes (1 mm width), a Ni/Cu microheater, and CNTs/reduced graphene hybrid film. A photograph of highly flexible NO<sub>2</sub> gas sensor is presented in Fig. 1(b).

Figure 1(c) shows I–V curves for the reduced graphene film and CNTs (20 μm)/reduced graphene hybrid film supported on polyimide substrates measured by two-terminal method. Both devices exhibited linear and symmetric I–V curves, suggesting Ohmic contact between the films and Au electrodes. The estimated resistances were 493 kΩ for reduced graphene film and 331 Ω for CNTs/reduced graphene film, respectively. It is well known that oxygenated graphene films are usually insulating at room temperature, with resistance values on the order of tens of gigaohms (GΩ), due to the disruption of conjugated graphitic structure by epoxide and hydroxyl groups on either side of the graphene basal plane.<sup>9</sup> However, the resistance of graphene oxide can be

<sup>a)</sup>Electronic mail: sychoi@etri.re.kr.

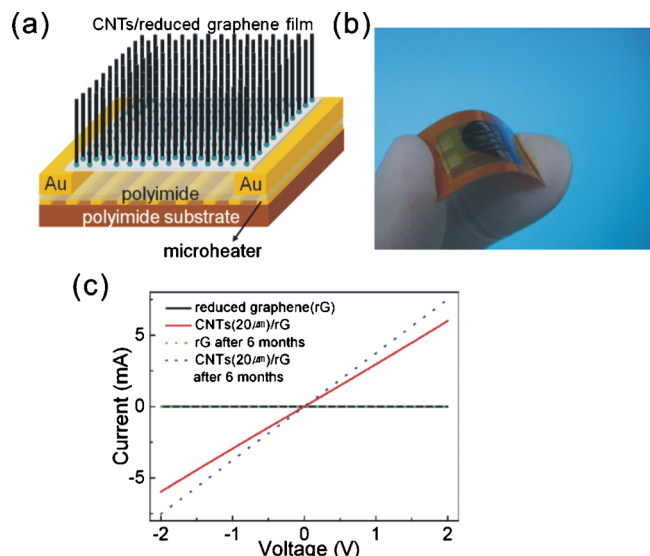


FIG. 1. (Color online) (a) A schematic illustration of the CNTs (20  $\mu\text{m}$ )/reduced graphene sensor device. (b) A photograph of the sensor device. (c) I-V curves for reduced graphene film and CNTs (20  $\mu\text{m}$ )/reduced graphene hybrid films transferred to polyimide substrates containing embedded Au electrodes. The dashed lines show the I-V curves measured after 6 months later.

reduced by thermal or chemical treatments that pyrolyse and remove the oxygen-containing functional groups.<sup>10</sup> In our thermal reduction approach, the reduced graphene films showed resistance values in the range of hundreds of kilohm. In contrast, the significantly decreased resistance of CNTs/reduced graphene hybrid films was clearly attributable to the highly conductive CNT arrays grown on the reduced graphene substrate. Our sensor device consisting of CNTs/reduced graphene hybrid film, therefore, can be considered as a parallel circuit containing a high resistance reduced graphene layer and a low resistance CNT array. The detailed electrical characterization of the hybrid films was reported in the previous report.<sup>8</sup>

Figure 2 shows typical  $\text{NO}_2$  sensing response signals from reduced graphene film and CNTs/reduced graphene hy-

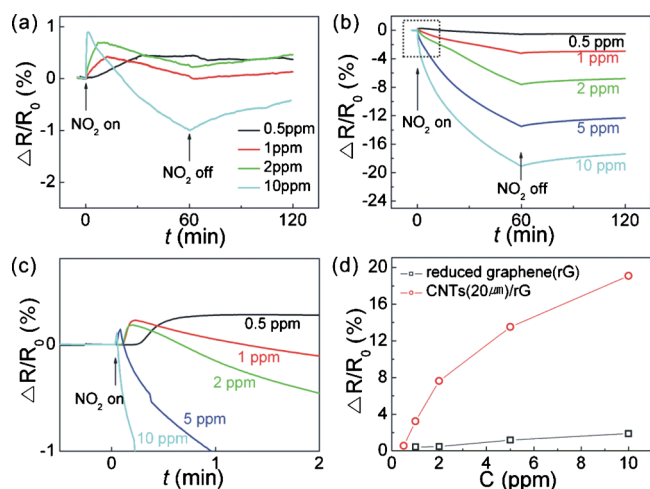


FIG. 2. (Color online) (a) Resistance variation in reduced graphene films upon exposure to various concentrations of  $\text{NO}_2$  gas. (b) Room-temperature  $\text{NO}_2$  sensing behavior of CNTs (20  $\mu\text{m}$ )/reduced graphene hybrid film devices at  $\text{NO}_2$  concentrations from 0.5 to 10 ppm. (c) A magnification of the region of (b) marked with dotted square. (d) Resistance response of reduced graphene and CNTs (20  $\mu\text{m}$ )/reduced graphene gas sensors measured after 60 min exposure to  $\text{NO}_2$  at various concentrations.

brid film devices operated at room temperature. The sensor device with CNT arrays without graphene was excluded in this experiment because it is still difficult to directly fabricate well-aligned CNTs on flexible substrates. The gas sensitivity ( $S$ ) was determined by  $S = (R - R_0)/R_0$ , where  $R_0$  is the initial resistance value measured in the presence of pure  $\text{N}_2$  and  $R$  is the resistance value measured in the presence of the  $\text{N}_2/\text{NO}_2$  gas mixture. The reduced graphene films exhibited a negligible sensing response at 10 ppm  $\text{NO}_2$ , as shown in Fig. 2(a). The response curves showed an unusual feature at all  $\text{NO}_2$  concentrations; the resistance increased in the beginning of  $\text{NO}_2$  exposure and subsequently decreased after several minutes. The degree of resistance increase depends on the  $\text{NO}_2$  concentration. The peak time for the highest resistance value became shorter as the  $\text{NO}_2$  concentration increased. Since reduced graphene films are known to behave as p-type semiconductors, this abnormal behavior could not be explained by the conventional p-type semiconductor space charge model that hole conduction is induced by an electron-withdrawing oxidizer, such as  $\text{NO}_2$ .<sup>3-5</sup> Instead, this unusual behavior was consistent with N-P transition behavior, which has been described in previous studies of oxide-based  $\text{NO}_2$  gas sensors.<sup>11,12</sup> The n-type characteristics of our reduced graphene films may have arisen from the growth conditions. Thermal treatment of the graphene oxide films took place in the presence of nitrogen.<sup>8</sup> Given that nitrogen-doped carbon-based materials generally behave as n-type semiconductor materials,<sup>13</sup> the observation of n-type semiconductor behavior during the initial injection of the oxidizing  $\text{NO}_2$  is reasonable for sensor devices containing as-grown reduced graphene films. Because graphene-based materials have a zero band gap,<sup>1</sup> a transition from n-type to p-type semiconducting behaviors can be induced by the absorption of electron withdrawing  $\text{NO}_2$  molecules. On the other hand, Lu *et al.*<sup>4</sup> proposed that the contact barrier modulation between Au electrode and reduced graphene film may induce the abnormal  $\text{NH}_3$  sensing behavior, showing a long-term nonlinear I-V behavior. The I-V curves for our devices after  $\sim 6$  months were shown as the dashed curves of Fig. 1(c). Because the curves were still symmetric and linear, which were almost consistent with that of the pristine device, we can exclude the contact issue from the cause of the abnormal  $\text{NO}_2$  sensing behaviors. The improved conductivity is probably caused by further-reducing of graphene substrate via the heating process during sensing measurements.

The reduced graphene only films did not show a prominent resistance change in response to introduction of  $\text{NO}_2$ . This poor sensitivity resulted from the residual presence of  $sp^3$ -hybridized carbons bearing hydroxyl or epoxide functional groups remaining after incomplete thermal reduction. According to recent reports on the fairly good performance of  $\text{NO}_2$  gas sensors based on reduced graphene and chemically derived graphene sheets,<sup>4,5</sup> the sensor response of our reduced graphene film device may be further optimized by modifying the graphene oxide reduction conditions. Meanwhile, the highly sensitive CNTs/reduced graphene hybrid films described here poses an alternative to the high cost graphene films. CNTs/reduced graphene films take advantage of the high sensing performance of CNTs and facile production of vertically aligned CNT arrays on reduced graphene surfaces.<sup>8</sup> The CNTs/reduced graphene hybrid films demonstrated remarkably enhanced sensitivity compared to reduced

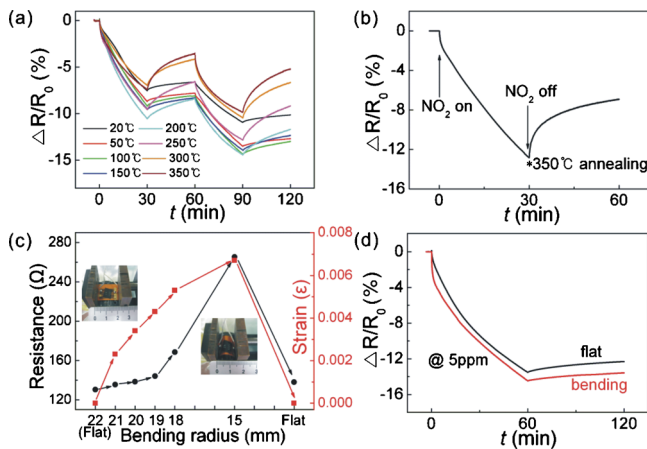


FIG. 3. (Color online) (a) Resistance variation in CNTs (20  $\mu\text{m}$ )/reduced graphene sensors to 5 ppm  $\text{NO}_2$  at various temperatures from 20 to 350  $^\circ\text{C}$ . (b) Sensor response curves for consecutive  $\text{NO}_2$  absorption and subsequent desorption assisted by microheater thermal treatment. (c) Resistance and strain variation in a CNTs (20  $\mu\text{m}$ )/reduced graphene hybrid film sensor device as a function of bending radius. The two insets show the bending apparatus. (d) Resistance responses of the flat and extremely bent (15 mm bending radius) devices to 5 ppm  $\text{NO}_2$  gas exposure.

graphene only films, as shown in Fig. 2(b). The variation in resistance was measured upon the exposure to  $\text{NO}_2$  concentrations ranging from 0.5 to 10 ppm. The CNTs/reduced graphene gas sensor responded to 10 ppm  $\text{NO}_2$  at room temperature with a sensitivity of 20% after 60 min exposure. The time–response curves, as a function of  $\text{NO}_2$  concentration, are plotted in Fig. 2(d), where the data were fit to an exponential rather than a linear model. The nonlinear sensitivity is supposed to be related to the vertical alignment of CNT arrays in the hybrid films. In the beginning of exposure, the  $\text{NO}_2$  gas molecules may attach at the upside of the vertical CNT arrays. Thereafter, they diffuse into the bottom perpendicular surfaces, resulting in a response different from those of horizontal nanowire sensors.<sup>6</sup> The unusual initial response peak in the measured resistance curves was also observed in the CNTs/reduced graphene films, as shown in Fig. 2(c), but the intensity of this peak was weaker than in the reduced graphene only film device.

Although a fast sensing response to  $\text{NO}_2$  gas was obtained for CNTs/reduced graphene sensor devices, the recovery rate was significantly slow. Usually, it took more than 60 min purging with  $\text{N}_2$  to recover the baseline signal. The temperature-dependence of the response to 5 ppm  $\text{NO}_2$  was measured, as plotted in Fig. 3(a). A Ni/Cu resistance microheater, insulated from the CNTs/reduced graphene film, was used for this measurement. The temperature varied from room temperature to 350  $^\circ\text{C}$ . The sensitivity increased with temperatures up to 200  $^\circ\text{C}$ , then decreased, indicating the existence of an optimal temperature. In contrast, the sensor recovery rate increased continuously with increasing temperature. These results imply that desorption of the gas molecules from the CNTs/reduced graphene films could be stimulated by thermal annealing using an embedded microheater. The gas desorption from the CNTs/reduced graphene gas sensor can, therefore, be effectively facilitated by use of microheater, after gas sensing at room temperature, as shown in Fig. 3(b).

The unique advantage of our sensor device is its mechanical flexibility, which arises from the combination of the polyimide substrate and the reduced graphene film substrate.

To demonstrate the stable operation of the  $\text{NO}_2$  gas sensor under bending stress, the sensor properties were measured as a function of bending radius. Figure 3(c) shows the resistance variation in a CNTs (20  $\mu\text{m}$ )/reduced graphene hybrid film with different bending radius and the corresponding top surface strains ( $\epsilon$ ), which were calculated using an equation given by Suo *et al.*<sup>14</sup> The resistance of the sensor device increased with the degree of bending. The recovery of the original resistance value was similar to the behavior, previously described for graphene only films.<sup>2</sup> Figure 3(d) shows the sensor response during extreme bending [bending radius of 15 mm in Fig. 3(c)] in the presence of 5 ppm  $\text{NO}_2$ . Interestingly, the sensing response was not significantly deteriorated.

In conclusion, a promising flexible  $\text{NO}_2$  gas sensor based on CNTs/reduced graphene hybrid films, was fabricated on polyimide flexible substrates containing an embedded microheater. In comparison with the reduced graphene films, CNTs/reduced graphene hybrid films showed remarkably enhanced sensitivity, which was attributed to the high sensitivity of vertically aligned CNT arrays. Thermal treatment by use of the Ni/Cu microheater embedded in the underlying polyimide substrate, facilitated the desorption of  $\text{NO}_2$  gas molecules, resulting in an enhanced recovery. In our work, without optimization of each component, high-performance flexible gas sensor was achieved by the synergistic combination of vertical CNT array and reduced graphene film substrate and the polyimide flexible substrate including microheater.

H.Y.J. and D.-S.L. contributed equally to this work. This work was supported by the basic research program of ETRI (Grant No. 10ZE1160) and the Pioneer Research Central Program (Grant No. 2009-0093758, NRF). S.O.K. acknowledges financial support from National Research Laboratory Program (Grant No. R0A-2008-000-20057-0, NRF).

- <sup>1</sup>K. S. Novoselov, A. K. Geim, S. V. Morozov, D. Jiang, Y. Zhang, S. V. Dubonos, I. V. Grigorieva, and A. A. Firsov, *Science* **306**, 666 (2004).
- <sup>2</sup>K. S. Kim, Y. Zhao, J. Jang, S. Y. Lee, J. M. Kim, K. S. Kim, J. Ahn, P. Kim, J. Choi, and B. H. Hong, *Nature (London)* **457**, 706 (2009).
- <sup>3</sup>F. Schedin, A. K. Geim, S. V. Morozov, E. W. Hill, P. Blake, M. I. Katsnelson, and K. S. Novoselov, *Nat. Mater.* **6**, 652 (2007).
- <sup>4</sup>G. Lu, L. E. Ocola, and J. Chen, *Nanotechnology* **20**, 445502 (2009).
- <sup>5</sup>J. D. Fowler, M. J. Allen, V. C. Tung, Y. Yang, R. B. Kaner, and B. H. Weiller, *ACS Nano* **3**, 301 (2009).
- <sup>6</sup>J. Kong, N. R. Franklin, C. Zhou, M. G. Chapline, S. Peng, K. Cho, and H. Dai, *Science* **287**, 622 (2000).
- <sup>7</sup>T. Zhang, S. Mubeen, N. V. Myung, and M. A. Deshusses, *Nanotechnology* **19**, 332001 (2008).
- <sup>8</sup>D. H. Lee, J. E. Kim, T. H. Han, J. W. Hwang, S. W. Jeon, S.-Y. Choi, S. H. Hong, W. J. Lee, R. S. Ruoff, and S. O. Kim, *Adv. Mater. (Weinheim, Ger.)* **22**, 1247 (2010).
- <sup>9</sup>W. Cai, R. D. Piner, F. J. Stadermann, S. Park, M. A. Shaibat, Y. Ishii, D. Yang, A. Velamakanni, S. J. An, M. Stoller, J. An, D. Chen, and R. S. Ruoff, *Science* **321**, 1815 (2008).
- <sup>10</sup>C. Gómez-Navarro, R. T. Weitz, A. M. Bittner, M. Scolari, A. Mews, M. Burghard, and K. Kern, *Nano Lett.* **7**, 3499 (2007).
- <sup>11</sup>Y. S. Kim, S.-C. Ha, K. Kim, S.-Y. Choi, H. Yang, J. T. Park, C. H. Lee, J. Choi, J. Paek, and K. Lee, *Appl. Phys. Lett.* **86**, 213105 (2005).
- <sup>12</sup>J. X. Wang, X. W. Sun, Y. Yang, and C. M. L. Wu, *Nanotechnology* **20**, 465501 (2009).
- <sup>13</sup>R. Czerw, M. Terrones, J.-C. Charlier, X. Blase, B. Foley, R. Kamalakaran, N. Grobert, H. Terrones, D. Tekleab, P. M. Ajayan, W. Blau, M. Rühle, and D. L. Carroll, *Nano Lett.* **1**, 457 (2001).
- <sup>14</sup>Z. Suo, E. Y. Ma, H. Gleskova, and S. Wagner, *Appl. Phys. Lett.* **74**, 1177 (1999).